Title

OPTICALLY DETECTED ADIABATIC INVERSION IN PHOSPHORESCENT TRIPLET STATES AND THE MEASUREMENT OF INTRAMOLECULAR ENERGY TRANSFER PROCESSES

Authors

Harris, C.B.
Hoover, Robert J.

Publication Date

1971-07-01

Submitted to Journal of Chemical Physics

LBL-118
Preprint

OPTICALLY DETECTED ADIABATIC INVERSION IN PHOSPHORESCENT TRIPLET STATES AND THE MEASUREMENT OF INTRAMOLECULAR ENERGY TRANSFER PROCESSES

C. B. Harris and Robert J. Hoover

July 1971

AEC Contract No. W-7405-eng-48

LAWRENCE RADIATION LABORATORY
UNIVERSITY of CALIFORNIA BERKELEY

DISCLAIMER

Optically Detected Adiabatic Inversion in Phosphorescent Triplet States and the Measurement of Intramolecular Energy Transfer Processes

by

C. B. Harris† and Robert J. Hoover

Department of Chemistry, University of California, and
Inorganic Materials Research Division, Lawrence Berkeley Laboratory,
Berkeley, California 94720

Abstract

The theory and observation of microwave induced population inversion within triplet magnetic sublevels in zero field are presented. It is shown that inversion via adiabatic fast passage can be measured quantitatively by changes in triplet phosphorescence and that population inversion can be accomplished easily and with microwave field strengths even lower than are required for saturation. Parameters affecting the ability to invert the sublevel populations such as dipolar interactions, microwave power and sweep rates are studied. General equations relating the intensity of phosphorescence and the fraction of inversion to

† Alfred P. Sloan Fellow

parameters associated with energy transfer processes into and from the triplet state such as intersystem crossing, radiative and radiationless relaxation are derived and measured for the $^3\pi\pi^*$ state of 2,3-dichloroquinoxaline. Additionally, time dependent kinetic equations which relate phosphorescence intensity changes to the microwave field and energy transfer parameters are derived. From these, the quantitative effects of the microwave field on the total ground and excited singlet state populations and the lowest triplet state population are determined. Finally, utilizing these results a new method for measuring absolute intersystem crossing rates and quantum yields from measurements of microwave induced changes in fluorescence is outlined.

I. Introduction

Optically detected magnetic resonance (ODMR) in zero field provides a powerful technique for investigating many different properties of aromatic and azaaromatic molecules in their triplet states.[1,2] A few parameters associated with electron distributions in excited triplet states such as the zero-field splitting of the magnetic sublevels, the nuclear-electron hyperfine and nuclear quadrupole coupling constants can be determined from an analysis of the fine structure in the EPR transitions.[2] In addition, techniques have evolved to determine other properties of the triplet state such as the rates and routes of intramolecular energy transfer.[1,3] Specifically, the intensity and polarization of phosphorescence can be modulated by connecting the magnetic sublevels of the triplet with a resonant microwave field.[4] Analysis of these changes makes it possible to determine the relative rates of intersystem crossing into the individual magnetic sublevels in addition to the radiative and radiationless decay rates from the sublevels to the ground state vibrational manifold. Several techniques have been developed to accomplish these ends. One, that described by van der Waals and co-workers,[3] relies on the fact that in many phosphorescent triplet states the total depletion rate (radiationless and radiative) from the individual magnetic sublevels are sufficiently different so that the population of one or more of the levels will be depleted much faster than the others upon extinguishing the exciting light. As a result, if a saturating microwave field equalizes the populations of two of the magnetic sublevels at various times after the exciting source is removed, population is transferred from the slower level to the partially depleted faster level resulting in a perturbation of the decaying phosphorescence intensity.

By analyzing the phosphorescence decay with and without the microwave perturbation the authors are able to effectively time resolve both the pre-exponential and exponential terms of the phosphorescence decay from all three of the magnetic sublevels. The sum of the radiationless and radiative decay rates are given by the exponential rate constants while the relative rates of intersystem crossing are reflected in the pre-exponential factors. A similar method has been reported by El-Sayed[1] in which the microwave field is left on during the full duration of the phosphorescence decay. In addition, El-Sayed has developed a steady state technique[1] utilizing continuous microwave saturation of the magnetic sublevels and continuous optical illumination. By using the steady state approximation in the quantitative interpretation of changes in the intensity of phosphorescence induced by the microwave field he is able to obtain the same rate constants.

Common to the above techniques are the assumptions that spin lattice relaxation between the magnetic sublevels is negligible and that saturation of the sublevels by the microwave field can both a) be achieved, and b) does not cause adverse effects such as heating or more subtle perturbations associated with strong rf fields. An additional assumption implied in the steady state approximation is that the populations of the excited singlet states are independent of any microwave perturbation.

A third method has been outlined[4] for the measurement of the relative rates of intersystem crossing; however, the details have not heretofore been presented. This method relies on the fact that inversion of the magnetic sublevel populations by adiabatic fast passage can be accomplished

with low microwave power and, more importantly, the fraction of inversion can be quantitatively measured. The virtue of this technique is that the population inversion can be applied under a variety of experimental conditions. Indeed, it can be used to eliminate the assumption of complete saturation in the decay techniques and steady state methods. In this way it can also be used to measure all the salient rate constants. It should be pointed out, however, that the adiabatic inversion method does not provide any additional new information beyond that obtainable from the other techniques but rather should be considered complimentary to them. The usefulness and accuracy of any one technique depends implicitly upon the detailed interplay of all of the rate constants of the specific molecule under investigation.

In the following sections of this paper the theory and observations of adiabatic inversion of the triplet magnetic sublevel populations in zero field will be presented. Next, the application of adiabatic inversion to the determination of all the rate processes associated with a phosphorescent triplet state will be developed and applied to the triplet $\pi\pi^*$ state of 2,3-dichloroquinoxaline doped in tetrachlorobenzene. Finally, equations for the transient behavior of phosphorescence induced by a microwave field will be developed. From these equations the manifestations of microwave induced excited singlet state population changes resulting from saturation effects will be discussed in the context of measuring magnetic resonance interactions via fluorescence (as opposed to phosphorescence) and the measurement of absolute intersystem crossing rates.

II. Optically Detected Adiabatic Inversion in Zero Field

In order to simplify the discussion of adiabatic inversion for a molecular triplet state in zero field in the presence of a linear polarized microwave field connecting two of the three magnetic sublevels we begin by transforming the spin Hamiltonian from the laboratory frame into an interaction representation in which the spin Hamiltonian reduces to a Zeeman interaction. In this representation adiabatic inversion of the magnetization will be equivalent to population inversion of the magnetic sublevels in the laboratory frame. Specifically, consider a total Hamiltonian, H_T, composed of the spin-dipolar zero-field Hamiltonian, H_{ss}, and a time dependent rf Hamiltonian, H_{rf}, connecting, for example, the τ_x and τ_y magnetic sublevels. In the laboratory frame such a Hamiltonian has the form

$$H_T = H_{ss} - 2\gamma H_1 \hbar \bar{S}_z \cos \omega t \qquad (1)$$

where γH_1 is the magnitude of the rf field, γ is the magnetogyric ratio of the electron, ω is the rf frequency and $\bar{S}_z$ is the magnetic dipole transition moment operator. The proper description of the spin system in the laboratory frame is given by the time dependent density matrix, ρ, where

$$\dot{\rho} = i/\hbar \, [\rho, H]. \qquad (2)$$

In the interaction representation the appropriate description of the spin system is again a time dependent density matrix ρ^*, where

$$\rho^* = U^{-1} \rho U, \qquad (3)$$

and

the unitary transformation U connecting the laboratory and interaction representation is given by

$$U = \exp(i\, G(t)/\hbar), \tag{4}$$

and the Hamiltonian, H^*, associated with ρ^* satisfies the following equations:

$$H^* = U^{-1} H_T U - (dG/dt)^* \tag{5}$$

$$\dot{\rho}^* = i/\hbar\, [\rho^*, H^*]. \tag{6}$$

The interaction representation can be viewed as a unitary transformation of the laboratory frame which removes the zero-field Hamiltonian provided the transformation matrix U is explicitly defined as

$$U = \exp(i\, H_{ss} \cdot t/\hbar). \tag{7}$$

Therefore it is clear that

$$H^* = -2\gamma H_1/\hbar \cos\omega t\; U^{-1} \bar{S}_z U, \tag{8}$$

and is nonsecular unless $\omega = (E_x - E_y)/\hbar$ where E_x and E_y are the appropriate eigenvalues of the zero-field Hamiltonian, H_{ss}. If we consider only a resonant microwave field then the interaction Hamiltonian becomes secular in first order at resonance and has the form of a Zeeman Hamiltonian in the rotating frame. Thus

$$H^* = -\hbar\gamma H_1 \bar{S}_z \ , \tag{9}$$

where the effective field γH_1 causes a "pseudo" magnetization to process around z. Stated in simplest terms, zero-field magnetic resonance of a triplet state can be viewed as that of an integral Zeeman spin system in its rotating coordinate frame.

The clarifying feature of this approach is that the motion of the magnetization in the interaction representation is equivalent to the dynamics of the zero-field alignment of the populations associated with the magnetic sublevels in the laboratory frame. For instance, it is well known that the magnetization of a Zeeman spin system can be inverted adiabatically by several methods. One, that using π pulses, requires H_1 fields that exceed the local dipolar field in order to insure that all spins are identically prepared in the time duration of the pulse. Another, adiabatic fast passage, follows directly from the adiabatic theorem which states that if the time variation of the effective field H_{eff} (in the present case $H_{eff} = \gamma H_1$) is slow enough, then the magnetization will follow the instantaneous effective field in the rotating frame. In addition, however, the conditions for fast passage in solids are determined in large measure by the local fields seen by the spin system. The presence of a dipolar spin system different from that associated with the resonant spin produces a local field, ΔH_{loc}, which, through magnetic dipole-dipole interactions, essentially adds to the effective field H_{eff}. If these local fields vary then the magnetization will follow the resultant field $H_{eff} + \Delta H_{loc}$; so unless the local fields are much smaller than the effective field and unless adiabatic inversion of the magnetization occurs faster than the relaxation time , adiabatic inversion will be incomplete. Ordinarily, adiabatic inversion is at best difficult in solids in high magnetic fields. A triplet state in zero field would not, however, be subject to the same restrictions as a spin system in high fields. The local dipolar field as seen by

the triplet states is expected to vanish in first order in the absence of an applied magnetic field. As a result, the contribution of the dipole-dipole terms to the linewidth vanishes and adiabatic inversion of the magnetization in the rotating frame or, equivalently, population inversion of the magnetic sublevels in the zero-field laboratory frame may be expected to occur at reasonably low H_1 fields. The reduction of the local field as seen by the triplet spin system -- dipolar quenching -- can be understood by analogy with the well-known quenching of integral nuclear spins in zero field[5] or the quenching of integral orbital angular momentum of electronic states.[6] Specifically, in the interaction representation the dipolar Hamiltonian contains only non-secular terms when no degeneracy associated with the spin eigenstates exists.[7] Consequently, in first order the coupling of the local dipolar field to the integral spin system vanishes in zero field. Applied to a triplet state in zero field, this means that when the molecule possesses an asymmetry around the principal zero-field tensor axis (i.e., the triplet has a finite E value) it may not be unreasonable to expect adiabatic inversion of the magnetic sublevel populations to occur at lower H_1 fields than are necessary for saturation. Indeed such has been observed in the phosphorescent triplet $\pi\pi^*$ state of 2,3-dichloroquinoxaline and other $n\pi^*$ and $\pi\pi^*$ aromatic triplet states.[8]

The experimental detection of adiabatic inversion in phosphorescent triplet states by optical means, i.e., monitoring the phosphorescences as a function of the microwave field, is relatively straightforward when rate processes associated with the individual magnetic spin sublevels are explicitly considered. It is well known that spin-orbit coupling

is selective for each of the triplet magnetic sublevels and thus quite often their radiative and radiationless rate constants differ in magnitude and/or polarization and their relative populations can be quite different. This means that changing the populations of the individual magnetic sublevels with a microwave field causes a change in the phosphorescent emission. Considering the intensity of emission from the magnetic sublevels as proportional to the rate times the population of the sublevels, the emission intensity to a particular vibronic level, I_o, is

$$I_o = \sum_{i=x,y,z} K_i N_i^\circ , \tag{10}$$

where individual magnetic sublevel radiative rate constants are K_i and the instantaneous populations are N_i°. If a microwave field is adiabatically swept through an electron spin transition, say $\tau_x \rightarrow \tau_y$, a certain fraction f of the population is transferred from one spin sublevel to the other and vice versa, while a fraction (1-f) is unchanged. This means that the population in the sublevels τ_x and τ_y after inversion are

$$N_x = (1-f)\, N_x^\circ + f\, N_y^\circ \tag{11}$$

$$N_y = (1-f)\, N_y^\circ + f\, N_x^\circ , \tag{12}$$

while τ_z remains unchanged. Consequently the intensity of phosphorescence after inversion becomes

$$I_1 = K_x[(1-f)N_x^\circ + f\, N_y^\circ] + K_y[(1-f)N_y^\circ + f\, N_x^\circ] + K_z N_z^\circ . \tag{13}$$

If the microwave field is swept through resonance a second time at a time τ after the first passage and if τ is short compared to radiative and radiationless relaxation processes, the population can again be altered, i.e.,

$$N_x = [1-2f+2f^2]N_x^\circ + [2f(1-f)]N_y^\circ \qquad (14)$$

$$N_y = [1-2f+2f^2]N_y^\circ + [2f(1-f)]N_x^\circ \ , \qquad (15)$$

and the phosphorescence intensity again changes to a value I_2 where

$$I_2 = K_x[(1-2f+2f^2)N_x^\circ + 2f(1-f)N_y^\circ] + K_y[(1-2f+2f^2)N_y^\circ + 2f(1-f)N_x^\circ] + K_z N_z^\circ \ . \qquad (16)$$

Using Equations (11-16) it is obvious that f, the fraction of inversion, is simply related to the measured phosphorescent intensities and is independent of both polarization effects and the populations associated with the τ_z sublevel. Thus the above equations yield

$$f = 1 - \tfrac{1}{2}\left[\frac{I_2-I_0}{I_1-I_0}\right] . \qquad (17)$$

It should be noted that in the event saturation is achieved, $f = \frac{1}{2}$, and the phosphorescence intensity is unchanged by the second inversion, that is, $I_1 = I_2$.

The above sequence is illustrated diagrammatically in Figure 1a and experimentally for 2,3-dichloroquinoxaline in Figure 1b. The details of Figure 1b are given in the experimental section. Figure 1b illustrates an obtainable f factor for adiabatic inversion via fast passage of 0.86.

The lack of a 100% inversion is probably in large measure due to the consequences of forbidden simultaneous nuclear-electron transitions. It is known[9] that the zero-field transitions of 2,3-dichloroquinoxaline consists of a manifold of states split by the N^{14} nuclear hyperfine and N^{14} nuclear quadrupole interactions. In the present case in addition to sweeping throughout the allowed transition we were forced, because of resolution difficulties, to sweep through several simultaneous N^{14} and electron spin transitions which have low ($\sim 10^{-1}$) transition moments. Consequently, the f factor is reduced from what it would be in the absence of these forbidden transitions. In all likelihood the electron-only transitions would have f's close to unity.

[Figure 1]

The ease of obtaining inversion points out the importance of dipolar quenching. This can be understood more completely from the conditions imposed by the adiabatic theorem. For complete inversion of the magnetization (or in the laboratory, population) in a system of free spins, the relationship between the applied field H_o in the presence of a radio-frequency field of frequency ω and magnitude H_1 and local dipolar fields, $\Delta H_{\ell oc}$ are

$$\frac{dH_T}{dt} = \frac{dH_o}{dt} < \gamma H_1^2 \qquad (18)$$

$$H_1 > \Delta H_{\ell oc} \; . \qquad (19)$$

Equation (18) is the adiabatic theorem and insures that the magnetization is always aligned along the instantaneous total field $H_T = H_o + H_1$. For a real spin system an additional requirement must be met. The adiabatic inversion must take place in a time short compared with any relaxation

processes in the spin system. Thus if τ is the time required for passage through resonance, then[10]

$$\tau \approx H_1 \frac{dH_o}{dt} < T_2 < T_1 , \qquad (20)$$

where T_1 and T_2 are the characteristic longitudinal and transverse relaxation times of the system. In a coordinate frame rotating about an applied field H_o at a frequency ω,

$$H_T = H_o + \frac{\omega}{\gamma} \qquad (21)$$

$$\frac{dH_T}{dt} = \frac{dH_o}{dt} + \frac{1}{\gamma}\frac{d\omega}{dt} \quad . \qquad (22)$$

In <u>zero</u> field, $\frac{dH_T}{dt} = \frac{1}{\gamma}\frac{d\omega}{dt}$; thus, adiabatic inversion can be accomplished by changing ω, the frequency of the applied RF field.

As was mentioned above, large fractions of inversion (> 80 per cent) are relatively easy to obtain. In an effort to determine the bounds of some of the quantities expressed in Equations (18-20), a study of the inversion factor as a function of H_1 and $\frac{dH_T}{dt}$ was made. A plot of f vs. dH_T/dt (or rather $d\omega/dt$) is shown in Figure 2. For these measurements the origin of the 2,3-dichloroquinoxaline phosphorescence was monitored while sweeping the applied microwave frequency through the 1.05 GHz resonance at various rates (0.1 to 40 milliseconds per 16 MHz), and using Equation (17) to determine f. One watt of rf power was used;

however, the actual power delivered to the sample was probably closer to 0.01 w. which corresponds to a field strength of approximately 0.1 gauss at the sample.[11] The important feature of Figure 2 is that adiabatic inversion can be accomplished with very long sweep times. A rough estimate of T_2 can be made utilizing Equation 20, i.e.,

$$\frac{T_2}{\Delta t} > \frac{2\gamma H_1}{\Delta \nu} \quad , \tag{23}$$

where a frequency $\Delta\nu$ was swept through in a time Δt. For $H_1 \sim 0.1$ gauss and $\Delta t = 40$ ms, $T_2 > 10^{-2}$ sec. This result is at first sight surprising since the EPR linewidths are ~1 MHz, which implies $T_2 \sim 10^{-6}$ sec. However, the T_2 in Equation (20) is the homogeneous T_2, while the linewidth is a sum of both a homogeneous T_2 and an inhomogeneous T_2^*, i.e., $\Delta\omega = \frac{1}{T_2} + \frac{1}{T_2^*}$. This result is qualitatively consistent with quenching of dipolar coupling for integer spin systems in zero field. The quenching can be removed by the application of an external magnetic field.[5] A study of the fraction of inversion as a function of an external magnetic field showed that f was reduced as anticipated from 0.93 in zero field to 0.5 in a 200 gauss field. To obtain another measure of T_2, one can estimate ΔH_{loc} via the condition implied by Equation (19). Figure 3b shows a plot of f vs. applied microwave power. Full power (0 dB) represents an rf field (H_1) of approximately 0.05 gauss. At approximately 10 dB attenuation ($H_1 = 5 \times 10^{-3}$ gauss) the inversion factor has been reduced to 0.5 (i.e., saturation). This implies local fields less than $\sim 5 \times 10^{-3}$ gauss, or a T_2 longer than $\sim 10^{-4}$ sec. This is in qualitative agreement with the aforementioned results for the dH/dt study.

[Figure 2]

[Figure 3]

The above data indicate that adiabatic inversion is, in general, easy to accomplish and consequently, as will be shown, it can be useful as a technique for determining triplet state parameters. In the following sections equations are derived which show how relative populations and intersystem crossing rate constants for the magnetic sublevels can be obtained from optically detected adiabatic inversion experiments. The method is then applied to 2,3-dichloroquinoxaline in tetrachlorobenzene.

III. Determination of Triplet State Parameters from Adiabatic Inversion Experiments

1. General Equations

The determination of the relative populations and intersystem crossing ratios of two triplet sublevels follows directly from Equations (10-17). Since the fraction of inversion, f, is determined via Equation 17 from a measurement of I_o, I_1 and I_2, one must determine population ratios using only I_o and I_1 or I_o and I_2, to avoid mathematical redundancy. Having determined f by Equation 17, the ratio of Equations 13 and 10 yields for population inversion of the x and y sublevels

$$\lambda^{xy} \equiv \frac{I_1^{x,y}}{I_o^{x,y}} = \frac{K_x[(1-f)N_x^o + f\,N_y^o] + K_y[(1-f)N_y^o + f\,N_x^o] + K_z N_z^o}{K_x N_x^o + K_y N_y^o + K_z N_z^o} \quad (24)$$

where the superscripts indicate which two levels were inverted. There are three such equations, one for each of the three zero-field transitions. Equation 24 contains six unknowns in addition to f; these are N_x^o, N_y^o, N_z^o, K_x, K_y and K_z. Therefore, for the most general case in which all three sublevels emit to the vibronic level being monitored, information from inversion experiments alone is insufficient to determine all parameters. However, the ratios $K_i N_i^o / K_i N_i^o$ are obtainable from a decomposition of the phosphorescence decay curve. These ratios combined with Equation 24 are sufficient to determine the relative triplet sublevel populations. For many triplet states not all of the magnetic sublevels are active to all vibronic bands. In such cases the equations become simplified. For a case where only one of the levels, say τ_y, emits, Equation 24 reduces to

$$\lambda^{xy} = \frac{K_y[(1-f)N_y^o + f\, N_x^o]}{K_y N_y^o} \quad . \tag{25}$$

Therefore,

$$\frac{N_x^o}{N_y^o} = \frac{\lambda^{xy}+f-1}{f} \quad , \tag{26}$$

and the population ratios are obtainable solely from adiabatic inversion measurements. In another special case where τ_x and τ_y emit to the monitored optical band, it is easily shown by defining ϵ as

$$\epsilon = \frac{I_2^{x,y}}{I_1^{x,y}} \quad , \tag{27}$$

that

$$\frac{N_x^o}{N_y^o} = \alpha = \left[\frac{\epsilon+1-2f-2(1-f)\lambda}{1-2f+\epsilon\lambda-2(1-f)\lambda}\right]^{\frac{1}{2}} , \tag{28}$$

and

$$\frac{K_y}{K_x} = \frac{(1-f-\lambda)\alpha+f}{\lambda+f(1-\alpha)-1} . \tag{29}$$

Thus adiabatic inversion data yield both population ratios and the radiative rate constant ratios for the two levels connected by the microwave field. The number of possible combinations of rate constants are too numerous to analyze individually; however, the method outlined above can be modified to accommodate other cases.

The above technique assumed that the time between inversions, τ, was small compared with the triplet state deactivation rates. It is not necessary to limit τ in such a manner (except to determine f accurately). General equations can be written to consider explicitly the decay processes which result from disturbing the steady state. This approach expresses the population of level i as a function of time and is given in the following equations:

$$N_i(t) = [N_i^o - N_i^e]\, e^{-k_i t} + N_i^e] , \tag{30}$$

where N_i^o is the population at $t = 0$, N_i^e is the equilibrium population at $t = \infty$ ($N_i^e = 0$ if no exciting light is present and $N_i = N_i^{ss}$, the steady state equilibrium population if exciting light is present) and k_i is the total decay rate of level i. For example, if $N_i^o = N_i^{ss}$ (i.e., the exciting light is left on), then for a case where $K_y \gg K_x, K_z$, and inverting levels τ_x and τ_y,

$$\lambda^{x,y}(t) = \frac{K_y\left[\left\{[(1-f)N_y^{ss} + fN_x^{ss}] - N_y^{ss}\right\}e^{-k_y t} + N_y^{ss}\right]}{K_y N_y^{ss}} \quad (31)$$

$$= 1 + f\left[\frac{N_x^{ss}}{N_y^{ss}} - 1\right] e^{-k_y t} \quad (32)$$

when inversion is performed at t = 0. Equation 32 reduces to Equation 26 for t = 0. Equation 32 can be expressed in terms of logarithms as

$$\ln\left\{\frac{\lambda(t)-1}{1}\right\} = \ln\left\{\frac{N_x^{ss}}{N_y^{ss}} - 1\right\} - k_y t \; . \quad (33)$$

A plot of Equation 33 gives the values k_y and $\frac{N_x^{ss}}{N_y^{ss}}$ more accurately in certain cases since one obtains many points as a function of t. Values for the steady state population ratios combined with triplet sublevel decay rates yield intersystem crossing ratios since

$$\frac{N_y^{ss}}{N_x^{ss}} = \frac{k_y^I}{k_x^I} \cdot \frac{k_x}{k_y} \quad (34)$$

where the k_i^I are the appropriate intersystem crossing rate constants.

A general requirement of the adiabatic inversion technique is that there be a reasonable population difference between the two levels being inverted since the change in the optical signal is proportional to $N_i - N_j$. This technique is applicable in any case where saturation experiments are useful and should be more sensitive. In the next section we apply the adiabatic fast passage population inversion technique to 2,3-dichloroquinoxaline in a tetrachlorobenzene host.

2. Application to 2,3-Dichloroquinoxaline

The optical and microwave spectra of 2,3-dichloroquinoxaline doped in durene have been analyzed by El-Sayed et al.[1,13] and Harris et al.[9] respectively. The corresponding spectra in a tetrachlorobenzene host are only slightly different. The zero-field level ordering and splittings are shown in Figure 4. Phosphorescence decay curves were obtained by monitoring either the origin (4679 Å) or the band at 4739 Å (0,0-260 cm^{-1}). Both bands decayed as single exponentials with decay rates of 5.77 sec^{-1} and 7.13 sec^{-1} respectively. This is consistent with the results in a durene host:[1] the 0,0 band originates from τ_z and the 0,0-260 cm^{-1} band originates from τ_y. A small amount of emission (~5%) was present in the origin which decayed with a lifetime of ~2 sec, which undoubtedly originates from τ_x, and again is consistent with the decay scheme[1] in a durene host. The similarity of dichloroquinoxaline in the two hosts is further supported by PMDR results in which a change in intensity of the origin is observed in the 1.05 GHz or 3.5 GHz transition but not for the 2.5 GHz transition. Likewise, the 0,0-260 cm^{-1} band is coupled only to the 2.5 GHz and 1.05 GHz EPR transitions. Thus, dichloroquinoxaline in tetrachlorobenzene is an easy test case for adiabatic inversion measurements since the simplified Equation 26 can be used insofar as one sublevel, to a good approximation, emits to each of the two abovementioned bands. Previous experiments[1] have shown that $N_x \approx N_y \approx 6N_z$ in a durene host. Since the relative triplet sublevel lifetimes are changed only slightly on going to a tetrachlorobenzene host, the same relative sublevel populations are expected as are found in a durene host. Inversion of the 1.05 GHz transition should

increase the intensity of the origin and decrease the intensity of the 0,0-260 cm^{-1} band by a factor of ~6. The observed changes given in Table I as I_1/I_o are about a factor of 7; thus, the population ratios obtained via adiabatic fast passage measurements are indeed close to those previously determined[1] by steady state methods. Using Equation 17, the fraction of inversion obtained in Figure 1b was 0.86. (Use of a better matched slow-wave helix yielded inversion fractions as high as 0.93.) The data obtained from identical inversion experiments utilizing the equations developed in Section II and all three zero-field transitions while monitoring the origin and 0,0-260 cm^{-1} band are summarized in Table 1. From the measured decay rates of τ_x and τ_y (5.77 and 7.13 sec^{-1} respectively) and the value $N_y/N_z = 8.00$, one obtains

$$\frac{k_y^I}{k_x^I} = 9.0 \quad .$$

This is lower than the value of ~15 reported by El-Sayed and Tinti[1] for the durene host. This reduction may be due to the external heavy atom effect of the tetrachlorobenzene host.. The above decay rates and intersystem crossing rates were used to calculate the predicted change in intensity of the origin upon saturation of the 1.05 GHz transition using Equation 12d of Reference 1. The intensity change was measured and found to be approximately 10% smaller than that predicted. This is consistent with the lack of complete saturation obtainable in this system. (See Section IV.)

[Table I]

Examination of Table 1 shows apparently inconsistent values for the N_y/N_z ratios obtained monitoring two different optical bands. The value obtained monitoring the 0,0-260 cm^{-1} band is inaccurate because the solution of Equation 26 accidentally gives in the numerator a small difference of two large numbers. Such unfortunate arithmetic did not occur in the evaluation of other ratios. Specifically, the experimentally determined N_y/N_x ratio obtained monitoring the 0,0-260 cm^{-1} band is close to that calculated from data obtained monitoring the origin. The ratios obtained by monitoring the origin were used in calculating the inter-system crossing ratios given above.

[Figure 4]

IV. Comparison of Adiabatic Inversion and Saturation Methods

The steady state methods[1] and decay methods[3] depend upon the ability to attain complete saturation of zero-field spin sublevels in order to quantitatively interpret the experimental results. Generally saturation is easily attainable in zero field at low temperatures, particularly if a high Q microwave cavity is used. However, depending upon the sample, the available microwave power and the cavity, saturation may not be possible. This is particularly true of low Q broad-banded slow wave helical cavities. Such a case is illustrated in Figure 3a which shows the phosphorescence intensity (origin) of 2,3-dichloroquinoxaline as a function of power while saturating the 1.05 GHz zero-field transition.

The lack of a plateau at high power clearly indicates incomplete saturation. The same saturation curves were obtained when the microwave field was modulated over the entire linewidth implying the lack of saturation is not due to the lack of spin diffusion. Figure 3b shows the fraction of inversion for the same transition using the same power and sample. It is apparent that inversion fractions greater than 0.5 are attainable at power levels at least a hundred times smaller than required for saturation; thus, the relative ease of adiabatic inversion may make it a preferred technique in some cases. An additional limitation of saturation techniques which require high continuous power is lack of temperature control due to heat dissipated in the sample. Since power need only be applied to the sample during passage through resonance in an adiabatic inversion experiment (see Experimental Section below), the rms power dissipated in the sample can be reduced by many orders of magnitude. A further difficulty can arise in the application of saturation methods to molecules with very short lifetimes due to the inability to saturate within a lifetime. Adiabatic inversion techniques may prove to be a better method in such cases. A general advantage of the inversion method is that populations can be sampled in a very short time -- e.g., microseconds. Another (usually) very small source of error in saturation experiments is the microwave effect on the singlet and ground state populations at saturation. (See Section V.) Because adiabatic fast passage experiments can be accomplished on a time scale much shorter than triplet state decay times, any change in relative triplet sublevel populations cannot be communicated to the ground state and thus to the excited singlet state by reabsorption.

In summary, saturation experiments are a useful and powerful technique in the library of optically detected magnetic resonance methods; however, in certain specific cases caution is necessary. Adiabatic inversion provides a complimentary technique useful in eliminating many of the potential sources of error in saturation and decay methods.

V. General Rate Equations Including Microwave Pumping

1. Time dependent populations

In section III the general equations relating to adiabatic inversion and the determination of intramolecular energy transfer parameters such as intersystem crossing ratios to the individual sublevels and sublevel populations were developed within the steady state approximation. It is not necessary, however, to assume steady state. In fact, relaxation spectra of the phosphorescence after the sublevel populations have been disturbed from steady state by a microwave field can be useful and powerful for the determination of kinetic parameters. This was briefly touched upon in Section III but not fully explored. It is precisely the transient features of the microwave induced phosphorescence which account for differences in signal intensity in CW vs. amplitude modulated optically detected magnetic resonance phenomena. A set of general rate equations are developed in this Section which describes more fully the time evolution of the triplet sublevel populations in the presence of continuous saturating microwave power. These equations not only describe the dynamics associated with kinetic parameters of the triplet state but also are useful in elucidating

what explicit features of the triplet state rate constants are important in determining the sensitivity of various optical microwave double resonance techniques.

The following discussion will use the following symbols and associated definitions.

N_x, N_y, N_z : triplet sublevel populations

N_s, N_G : excited singlet and ground state populations

k_i, i = x,y,z: sum of radiative and non-radiative rate constants for the triplet sublevels

k_i^I, i = x,y,z: intersystem crossing rates to triplet sublevels

k_s' : radiative rate constant ($1/\tau$) of singlet state used for excitation

k_s : sum of radiative and radiationless (excluding Isc) rate constants of the lowest singlet state

I : rate of absorption of photons for the transition used for excitation

The time rate of change for the magnetic sublevel populations connected by a saturating microwave field in the absence of spin lattice relaxation are:

$$\frac{dN_x}{dt} = k_x^I N_s - k_x N_x + W(N_y - N_x) \qquad (35a)$$

$$\frac{dN_y}{dt} = k_y^I N_s - k_y N_y + W(N_x - N_y) \qquad (35b)$$

W is the microwave pumping rate which is determined by the transition probability and applied microwave power. Solution of these two equations yields

$$N_x(t) = C_1 e^{r_1 t} + C_2 e^{r_2 t} + C_3 , \tag{36a}$$

$$N_y(t) = C_4 e^{r_1 t} + C_5 e^{r_2 t} + C_6 , \tag{36b}$$

$$r_1 = -\tfrac{1}{2}[(k_x+k_y) + 2W] + \tfrac{1}{2}[(k_x-k_y)^2 + 4W^2]^{\frac{1}{2}} , \tag{37}$$

$$r_2 = -\tfrac{1}{2}[(k_x+k_y) + 2W] - \tfrac{1}{2}[(k_x-k_y)^2 + 4W^2]^{\frac{1}{2}} . \tag{38}$$

The C_i's are constants determined by initial boundary conditions. For high microwave power, $W \gg k_x, k_y$ and

$$r_1 = -\tfrac{1}{2}(k_x+k_y), \tag{39}$$

$$r_2 = -2W . \tag{40}$$

If the microwave power is turned on and exciting light is removed at $t = 0$ and if

$$N_x(0) = N_x^o \quad \text{and} \quad N_y(0) = N_y^o ,$$

then

$$N_x(t) = \tfrac{1}{2}(N_x^o + N_y^o)\, e^{-\frac{1}{2}(k_x+k_y)t} + \tfrac{1}{2}(N_x^o - N_y^o)\, e^{-2Wt} , \tag{41}$$

$$N_y(t) = \tfrac{1}{2}(N_x^o + N_y^o)\, e^{-\frac{1}{2}(k_x+k_y)t} + \tfrac{1}{2}(N_y^o - N_x^o)\, e^{-2Wt} . \tag{42}$$

The second term on the right hand side of Equations 41 and 42 is a transient effect which tends to equalize N_x and N_y. At high microwave powers, however, this effect is very fast, 10^{-6} sec; consequently at times longer

than $\sim 10^{-6}$ sec. Equations 41 and 42 describe a decay experiment. Specifically when the exciting light is shut off and saturating microwave power is turned on at t = 0, after equilibration each level decays with a rate constant which is the average of the rate constants of the sublevels in the absence of microwave power.

In the case where the sample is constantly irradiated with exciting light and microwave power is turned on, the populations of the two levels are equalized at the end of the equilibration time, i.e., $N_x = N_y = \frac{1}{2}(N_x^o + N_y^o)$; however, the total population evolves in time because the system is no longer at steady state. The change which takes place is on a time scale comparable to the triplet state lifetime. Specifically, the total population of the two levels connected by the microwave field assuming that the sublevel populations are equal at t = 0 is given by

$$N_T(t) = \left\{ \left[\frac{k_x^I}{k_x} + \frac{k_y^I}{k_y} - \frac{k_x^I + k_y^I}{\frac{1}{2}(k_x+k_y)} \right] e^{-\frac{1}{2}(k_x+k_y)t} + \frac{k_x^I + k_Y^I}{\frac{1}{2}(k_x+k_y)} \right\} N_s \quad (43)$$

and $N_x = N_y = \frac{1}{2}N_T$. This equation assumes negligible change in the singlet state population upon microwave saturation. Although this equation is not exact for $t \to \infty$ because we are neglecting any singlet state population changes, it is useful in that it describes the time evolution to a new steady state. Thus

$$N_T(\infty) = 2\frac{(k_x^I + k_y^I)}{(k_x + k_y)} N_s \quad (44)$$

and

$$\frac{N_T(\infty)}{N_T(0)} = \frac{2(k_x^I + k_y^I)}{(k_x + k_y)} \left[\frac{k_x^I}{k_x} + \frac{k_y^I}{k_y}\right]^{-1} , \tag{45}$$

$$\frac{N_{x,y}(\infty)}{N_x(0)} = \frac{(k_x^I + k_y^I)}{(k_x + k_y)} \cdot \frac{k_{x,y}}{k_{x,y}^I} . \tag{46}$$

Equation 46 is identical to that given by El-Sayed.[1] The values at $t = \infty$ are the new steady state saturation values resulting from the microwave perturbation. Table II contains a summary of $N_T(\infty)$ values for various relative rate constants.

[Table II]

Figure 5 summarizes some of the results of Table II and illustrates the time evolving population of the sublevels. From Figure 5 it is apparent when an amplitude modulated experiment will be more sensitive than a CW experiment. When the phosphorescence returns to a value near its value in the absence of microwave power after the initial transient decay or build-up, then the steady state value in the presence of microwaves is almost equal to that in the absence; consequently the CW detected signal is weak. On the other hand, because of the sizeable transient at the start of the applied field, standard AM phase detection is likely to yield large signals.

2. Steady State Population Changes Induced by Microwave Saturation

The above derivation has neglected any effects on the steady state excited singlet state populations resulting from changes in the triplet state populations being communicated to the excited singlet states by reabsorption. In dilute samples where the microwave field causes a large shift in the steady state triplet population, the singlet population can be changed under certain circumstances. In this section, expressions for the steady state singlet and triplet state population under continuous optical excitation are derived. It will be demonstrated under what conditions changes in excited singlet state populations occur upon saturation of the triplet spin sublevels with a microwave field, and how this phenomenon can lead to the fluorescence detection of microwave transitions.

Using the following additional definitions:

N_o : total number of molecules in the sample

k^I : $\sum_i k_i^I$

N_T : $N_x + N_y + N_z$,

the populations N_i are governed by the following equations:

$$\frac{dN_s}{dt} = I\, N_G - (k^I + k_s)\, N_s \tag{47}$$

$$\frac{dN(x,y,z)}{dt} = k^I(x,y,z)\, N_s - k(x,y,z)\, N(x,y,z) \tag{48}$$

$$\frac{dN_G}{dt} = - I N_G + k_x N_x + k_y N_y + k_z N_z + K_s N_s \quad . \qquad (49)$$

At steady state the above derivatives are equal to zero. Therefore, from Equation 48

$$N(x,y,z) = \frac{k^I(x,y,z)}{k(x,y,z)} N_s \quad . \qquad (50)$$

Using Equation 50 it is easily shown that

$$k_x N_x + k_y N_y + k_z N_z = \Gamma N_T \quad , \qquad (51)$$

where

$$\Gamma = \frac{\Sigma_i k_i^I}{\Sigma_i k_i^I / k_i} \quad . \qquad (52)$$

Equations 47-49 can be rewritten in terms of N_T by use of Equation 51 and thus, at steady state

$$I N_G - (k^I + k_s) N_s = 0 \qquad (53a)$$

$$I N_G + k_s N_s + \Gamma N_T = 0 \qquad (53b)$$

$$N_G + N_s + N_T = N_o \quad . \qquad (53c)$$

Solution of Equations 53 gives

$$N_T = \beta N_o \qquad (54)$$

$$N_s = \frac{\Gamma}{k^I} \beta N_o \qquad (55)$$

$$N_G = \left\{ \frac{\Gamma}{I} \frac{k_s}{k_I} + 1 \right\} \beta N_o \quad , \qquad (56)$$

where

$$\beta = \left[\frac{\Gamma}{I}\left\{\frac{k_s}{k^I} + 1\right\} + \frac{\Gamma}{k^I} + 1\right]^{-1} \quad . \tag{57}$$

An excitation source such as a PEK-100 watt Hg-Xe arc lamp gives I values of ~ 0.1 when exciting a singlet state which has an oscillator corresponding to a lifetime of 10^{-8} sec. This is typical of the lower singlet states of small aromatic hydrocarbons and N-heterocycles. Taking typical values for molecular rate constants and taking a case where $k_x^I > k_y^I$ and $k_x > k_y$ such that $N_x/N_y \sim 10$, we find

$$\Gamma \approx 5,$$

$$\beta \approx 0.02;$$

thus from Equations 54 and 55

$$\frac{N_T}{N_o} \approx 0.076$$

$$\frac{N_s}{N_o} \approx 7.6 \times 10^{-9} \quad .$$

Upon microwave saturation of the $\tau_x \rightarrow \tau_y$ transition

$$\bar{k}_x \equiv \bar{k}_y = \tfrac{1}{2}(k_x + k_y)$$

and

$$\bar{k}_x^I \equiv \bar{k}_y^I = \tfrac{1}{2}(k_x^I + k_y^I) \quad .$$

The overbars are the effective rate constants in the presence of a microwave field. This substitution is possible since under saturation

$N_x = N_y$ and the appropriate rate constants are equal to the average of the rate constants for the two levels in the absence of a saturating microwave field. Therefore

$$\frac{\bar{N}_T}{N_o} = 0.016 ,$$

and

$$\frac{\bar{N}_s}{N_o} = 8 \times 10^{-9} .$$

Thus, the total triplet state population decreases by a factor of ~ 5 and lowest singlet state population increases by $\approx 5\%$ upon microwave saturation of the EPR transition. The magnitude of these changes are of course dependent upon the exact choice of rate constants used in the calculation. The important point is that a change in singlet state population of a per cent or so is readily measurable. This means that detection of zero-field ESR transitions via monitoring fluorescence is feasible. As was shown above (see Table II), there are certain possible combinations of triplet state rate constants which, if present, give a much larger change in the triplet state population upon microwave saturation than the factor of five mentioned above. In such cases large changes in the singlet state population can occur.

The quantitative interpretation of a change in fluorescence upon microwave saturation of the triplet magnetic sublevels can be used to determine individual intersystem crossing rates directly. Consider, for example, the case where intersystem crossing occurs to τ_y and only τ_y radiates to the ground state. We will neglect radiationless processes from τ_y. From Equation 55

$$\frac{N_s}{\bar{N}_s} = \frac{\Gamma\beta}{\bar{\Gamma}\bar{\beta}}$$

$$\Gamma = k_y$$

$$\bar{\Gamma} = \tfrac{1}{2}k_y$$

$$\frac{N_s}{\bar{N}_s} = 2\,\frac{\beta}{\bar{\beta}} \quad . \tag{58}$$

Using Equations 57 and 58, and defining $\mu = 2\,\frac{N_s}{\bar{N}_s}$,

$$k_y^I = (\mu-1)\left\{\frac{k_s}{I} + 1\right\}\left\{\frac{2-\mu}{k_y} + \frac{(1-\mu)}{I}\right\}^{-1} \quad . \tag{59}$$

Thus, k_y^I is obtainable directly from a knowledge of fluorescence and phosphorescence lifetimes in addition to the intensity of exciting light. If intersystem crossing occurs to all sublevels, then three simultaneous equations must be solved, each one utilizing saturation of one of the three zero-field transitions.

This technique is useful only if a measurable change in singlet state population occurs and can be monitored via fluorescnece. Under favorable circumstances, this method could be used to measure absolute rate constants. It alleviates many of the complications of quantum yield measurements such as the integration of the emission over the spectra and phototube calibrations since all measurements can be made at one wavelength and calibration of the exciting light intensity is reasonably straightforward. Thus, in certain cases this method may be easier and more accurate than those presently employed.

VI. Experimental

Samples of 1,2,4,5-tetrachlorobenzene and 2,3-dichloroquinoxaline were purified by repeated zone refining (200 passes at 2 hours per pass) and recrystallization followed by vacuum sublimation, respectively. A single crystal sample of 2,3-dichloroquinoxaline in tetrachlorobenzene ($\sim 10^{-3}$ m/m) was grown by standard Bridgeman technique. Microwave power was obtained from a Hewlett-Packard Model 8690-B sweep oscillator used in conjunction with a Servo Corp. Model 2220 Microwave power amplifier. AM and FM modulation signals for the sweep oscillator were obtained from a General Radio type 1395-A pulse generator. Microwave power was applied to the sample through a rigid coaxial line terminated with a slow wave helix. The sample was suspended in a liquid helium dewar with the sample in contact with liquid helium. Temperatures below 4.2°K were obtained by pumping on the liquid helium. Phosphorescence was detected through a Jarrell-Ash 3/4 M Czerney-Turner spectrograph. Light from a PEK-100 watt mercury arc lamp was focused through a water filter and a Schott 3100 Å interference filter for excitation. A block diagram of the experimental setup is shown in Figure 6. All measurements were made at 1.35°K.

[Figure 6]

The frequency sweep required to invert the triplet sublevels was obtained by applying a ramp voltage to the F.M. input of the microwave sweep generator. The ramp voltage (V) was adjusted so that when $V = V_o$, the microwave frequency was ω_o, the center of the EPR transition

being used for inversion (see Table I and Figure 7). The FM voltage was swept linearly from $V_o - \frac{1}{2}v$ to $V_o + \frac{1}{2}v$ in a time τ so that the microwave frequency change from $\omega_o - \frac{1}{2}\delta$ to $\omega_o + \frac{1}{2}\delta$ (see Table I) in a time τ. After a time Δ, the frequency was swept back from $\omega_o + \frac{1}{2}\delta$ to $\omega_o - \frac{1}{2}\delta$. Thus by varying τ and fixing δ one varies dH/dt (Eq. 22). The data in Fig. 2 was obtained by varying τ from 0.1 to 40 milliseconds. To obtain the best signal-to-noise ratio the inversion was performed at 4-second intervals (to allow reestablishment of steady-state conditions), each inversion signal being fed into a PAR Waveform Eductor. This averaging technique greatly improved signal-to-noise ratios over simply photographing one sample displayed on an oscilloscope. This method was used for the inversion measurements, (Fig. 2,3) the saturation measurements shown in Fig. 3, and phosphorescence lifetime measurements. To minimize any heating effects, microwave power was applied to the sample only during passage through resonance. Microwave power was applied by using an offset squarewave pulse to the AM input of the microwave sweeper.

[Figure 7]

The time between inversions, Δ, (see Fig. 7), was zero for the 10, 20 and 40 ms points in Figure 2, and 0.5 ms for all other data. The values of δ for the three zero-field transitions are listed in Table I. The microwave sweeper could follow FM signals which produced a change of 10 MHz in 80 μsec. Thus to insure linearity in the frequency sweep, τ values below 100 μsec were not used. Since the total time for determining f values ($2\tau + \Delta$, Fig. 7) was 0.7 ms and the phosphorescence

lifetimes of the 2,3-dichloroquinoxaline are ~ 100 ms, errors introduced by triplet decay and intersystem crossing were negligible in the determination of the triplet sublevel populations and intersystem crossing rates (Table I).

The power level changes for the data in Fig. 3 were made by inserting Hewlett-Packard precision microwave power attenuators in the transmission line.

VII. Acknowledgments

This work was supported by the Inorganic Materials Research Division of the Lawrence Berkeley Laboratory under the auspices of the U.S. Atomic Energy Commission.

Table I

Summary of Experimental Adiabatic Fast Passage Inversion Results for 2,3-dichloroquinoxaline

0,0-Band

ω_o [a]	f [b]	I_1/I_o [c]	δ [d]	Power [e]	N_y°/N_z°	N_y°/N_x°	N_x°/N_z°
1.05	0.88	7.15	16	1.2	8.00	-	-
2.45 [h]	0	-	-	-	-	3.47 [f]	-
3.50	0.85	2.20	30	1.0	-	-	2.30

0,0-260 cm^{-1} Band

1.05	0.90	0.166	16	1.2	13.5 [g]	-	-
2.45	0.81	0.56	4	10.0	-	3.50	-
3.50 [h]	0	-	-	-	-	-	3.8 [f]

[a] Zero-field transition used for inversion, GHz.

[b] Fraction of inversion obtained.

[c] Ratio of phosphorescence intensities after and before inversion.

[d] Frequency range swept through to obtain inversion - a sweep time of 100 μsec was used (see experimental section), MHz.

[e] Applied power, watts: one watt gives an effective field of approximately 0.1 gauss.

[f] This value is obtained from the ratio of the two other ratios.

[g] This value is very uncertain because in applying Eq.26 the numerator results from the subtraction of two large numbers to yield a small number with a consequently high error.

[h] Excitation of this zero field transition produces no change in phosphorescence intensity.

Table II

Summary of Triplet Sublevel Population Changes Upon Microwave Saturation

k_x/k_y [a]	k_x^I/k_y^I	N_x^o/N_y^o	$\bar{N}_T(\infty)/N_T(0)$	$\bar{N}_x(\infty) = \bar{N}_y(\infty)$	Illustrated in Figure:
1	≥ 1	≥ 1	1	$\frac{1}{2}(N_x^o + N_y^o)$	5a
1	≤ 1	≤ 1	1	$\frac{1}{2}(N_x^o + N_y^o)$	5a
	1		$4k_xk_y/(k_x+k_y)^2$		5b
$\gg 1$	1	$\gg 1$	$4k_y/k_x \ll 1$	$2N_y^o \ll N_x^o$	5b
	$\gg 1$	$\gg 1$	2	$N_x^o \gg N_y^o$	5c
$\ll 1$	$\gg 1$		$2k_x/k_y \ll 1$	$k_x/k_y\ N_x^o \ll N_x^o$	5d

[a] See text for definition of symbols.

References

1. For a review of the determination of triplet state parameters via ODMR techniques see D. S. Tinti and M. A. El-Sayed, J. Chem. Phys. 54, 2529 (1971), and references therein.
2. For a review of ODMR in zero field see M. J. Buckley and C. B. Harris, J. Phys. Chem. XX, XXXX (1971), and references therein.
3. J. Schmidt, W. S. Veeman and J. H. van der Waals, Chem. Phys. Letters 4, 341 (1969).
4. C. B. Harris, J. Chem. Phys. 54, 972 (1971); Proc. of the 5th Molecular Crystal Symposium, Philadelphia (1970).
5. G. W. Leppelmeier and E. L. Hahn, Phys. Rev. 141, 724 (1966).
6. J. H. van Vleck, Phys. Rev. 74, 1168 (1948).
7. M. Schwab and E. L. Hahn, J. Chem. Phys. 52, 3152 (1970).
8. M. J. Buckley, C. B. Harris and R. M. Panos, unpublished results.
9. C. B. Harris, D. S. Tinti, M. A. El-Sayed and A. H. Maki, Chem. Phys. Letters 4, 409 (1969).
10. A. Abragam, "The Principles of Nuclear Magnetism," Oxford University Press, London, 1961, p. 554.
11. Microwave field strength measurements are obtainable from inversion experiments using π-pulses.[4] Experiments similar to those reported by Schmidt *et al.*[15] were performed and a measure of H_1 obtained (see Eq. 12 of Ref. 4a and Eq. 11 of Ref. 15).
12. M. A. El-Sayed, J. Chem. Phys. 54, 680 (1971).

13. M. A. El-Sayed, D. S. Tinti and D. Owens, Chem. Phys. Letters 3, 339 (1969).

14. C. B. Harris and Robert J.Hoover, unpublished results.

15. J. Schmidt, V. C. van Dorp, and J. H. van der Waals, Chem. Phys. Letters 8, 345 (1971).

Figure Captions

Figure 1. (a) Schematic representation of the phosphorescence intensity change produced by inverting the populations of two magnetic triplet sublevels. The phosphorescence originates from the level having the smaller steady state population in the illustration. The intensity increases to the value at (1) upon inversion. After a short time the populations are inverted again and the phosphorescence intensity changes to the value at (2). The value at (2) is larger than the intitial steady state value because the fraction of inversion (see text) is less than unity. The dashed line shows decay due to radiative and non-radiative processes. (b) Oscilloscope tracing of the phosphorescence origin of 2,3-dichloroquinoxaline in a tetrachlorobenzene host while inverting the populations of the τ_y and τ_z sublevels by sweeping through the 1.05 GHz ESR transitions. The time between inversions was 10 ms; a fraction of inversion of 0.86 was obtained.

Figure 2. Plot of the fraction of inversion in 2,3-dichloroquinoxaline as a function of the time (τ) required to sweep through resonance. The fraction of inversion is highest for short sweep time (i.e., large dH/dt) because the "forbidden" electron-nuclear transitions cannot follow the changing field and hence cannot reduce the fraction of inversion as explained in the text.

Figure 3. (a) Phosphorescence intensity of 2,3-dichloroquinoxaline as a function of applied microwave power. The non-uniform shape of the curve is probably due to the power-dependence of the mode pattern inside the helical slow-wave cavity. (b) Plot of the fraction of inversion vs. applied microwave power.

Figure 4. Energy level diagram of the lowest triplet state of 2,3-dichloroquinoxaline. Heavy arrows indicate the principal phosphorescence routes.

Figure 5. Triplet sublevel populations as a function of time after turning on a saturating microwave field. The populations are equilibrated in a time τ ($\tau \sim 10^{-6}$ sec) and then change to a new steady state value ($t = \infty$) with a time constant approximately equal to the triplet state lifetimes. The time ϕ represents a typical modulation period used in a.m. modulated experiments.

Figure 6. Block diagram of the experimental arrangement.

Figure 7. Time dependence of microwave frequency (ω) and power (P) (see text for details).

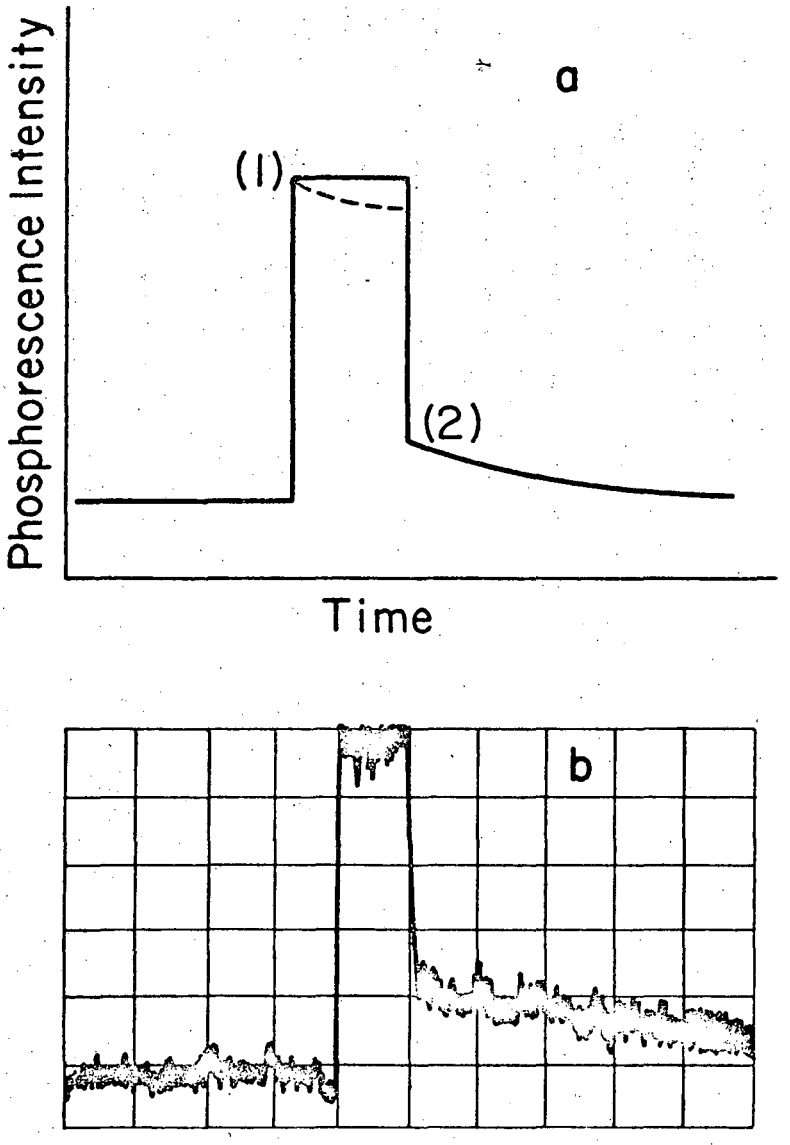

XBL 717-6926

Fig. 1

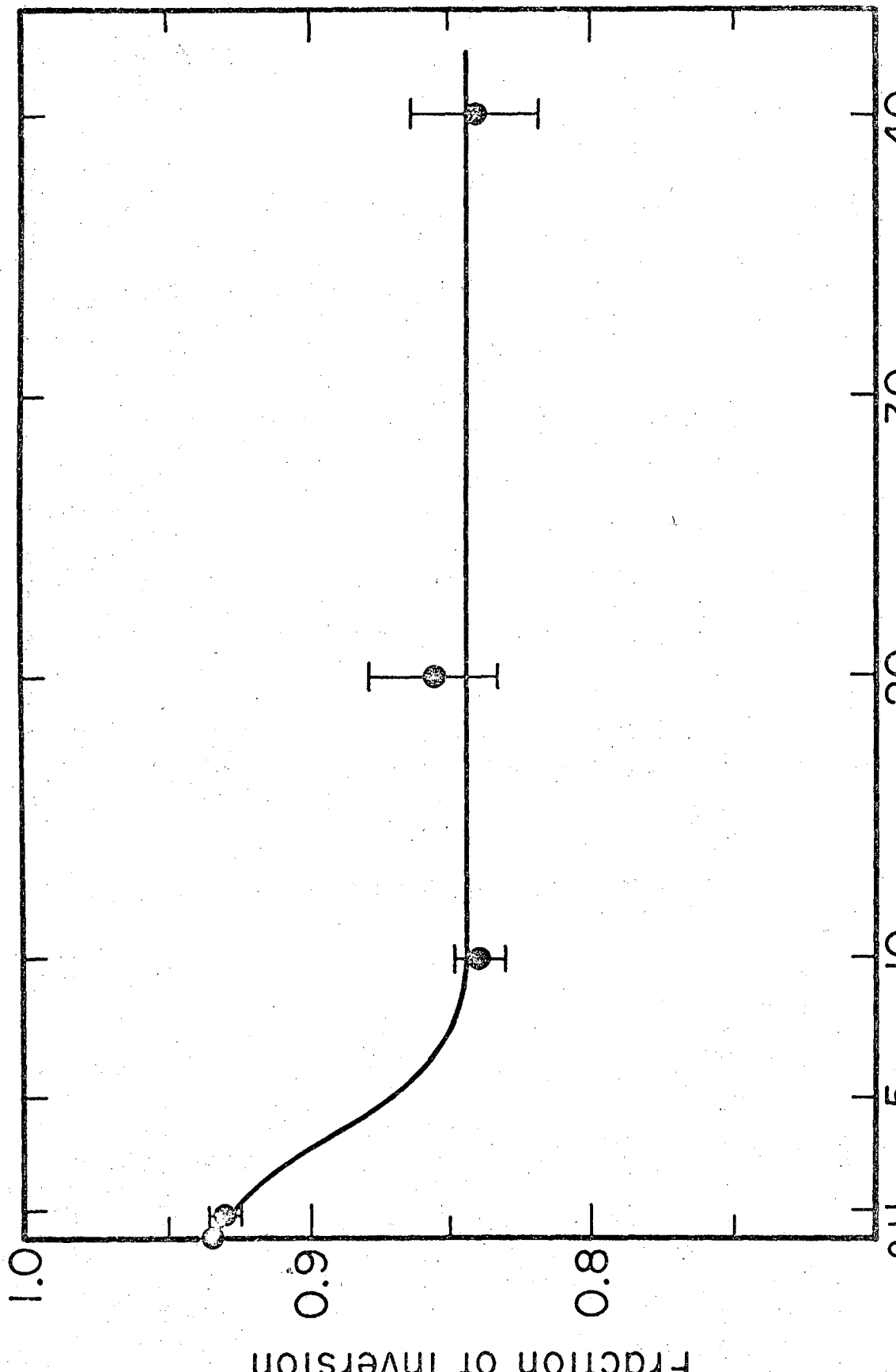

XBL 716-6896

Fig. 2

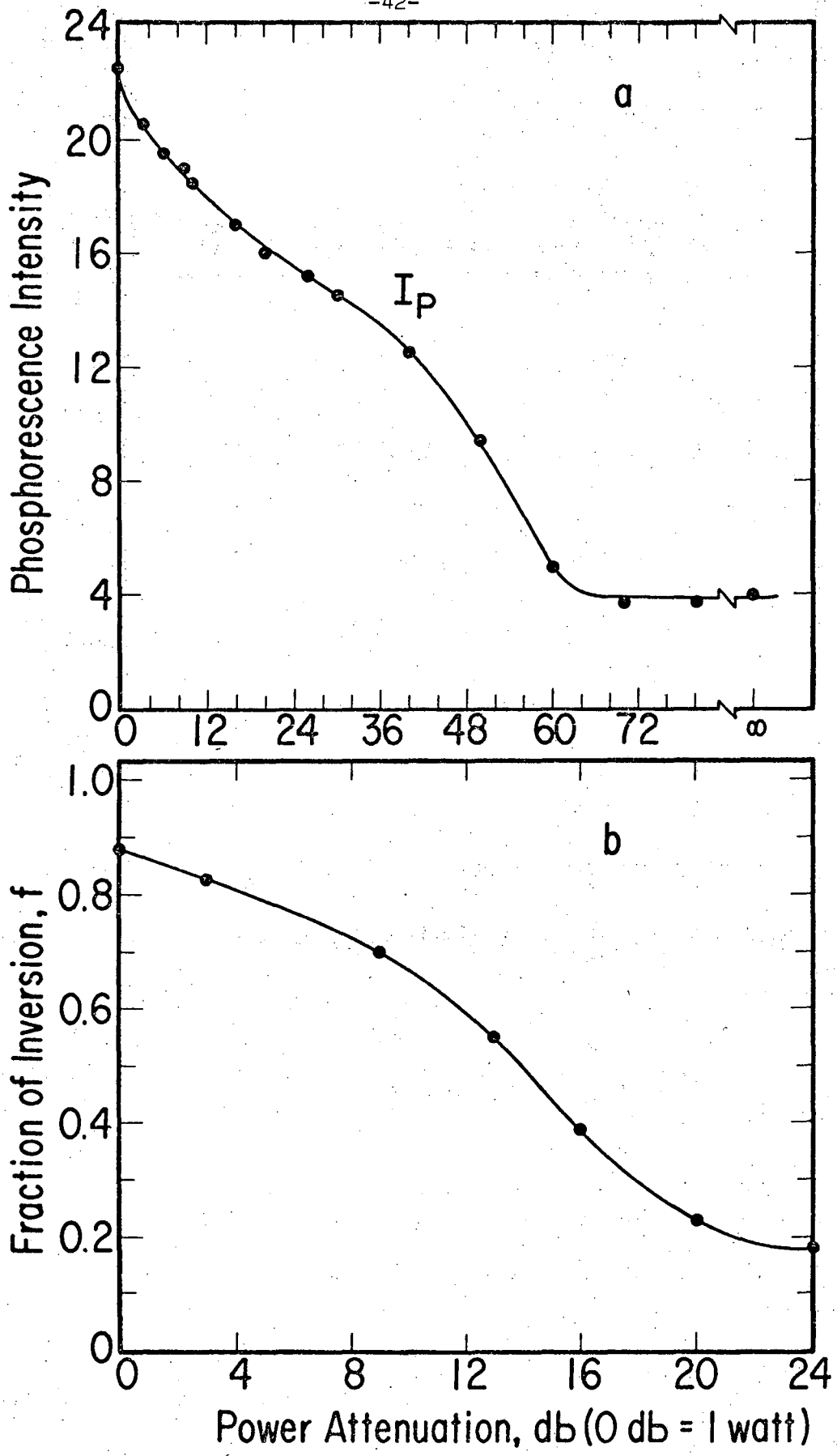

XBL 717-6925

Fig. 3

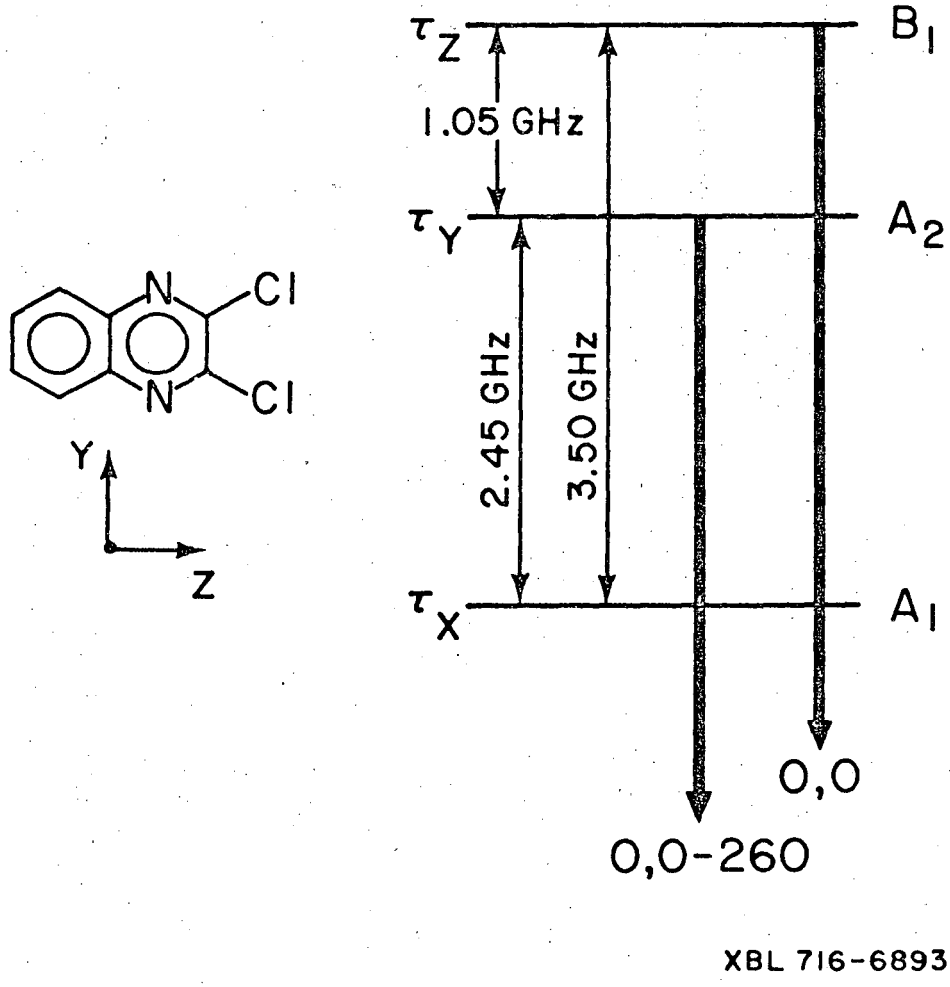

Fig. 4

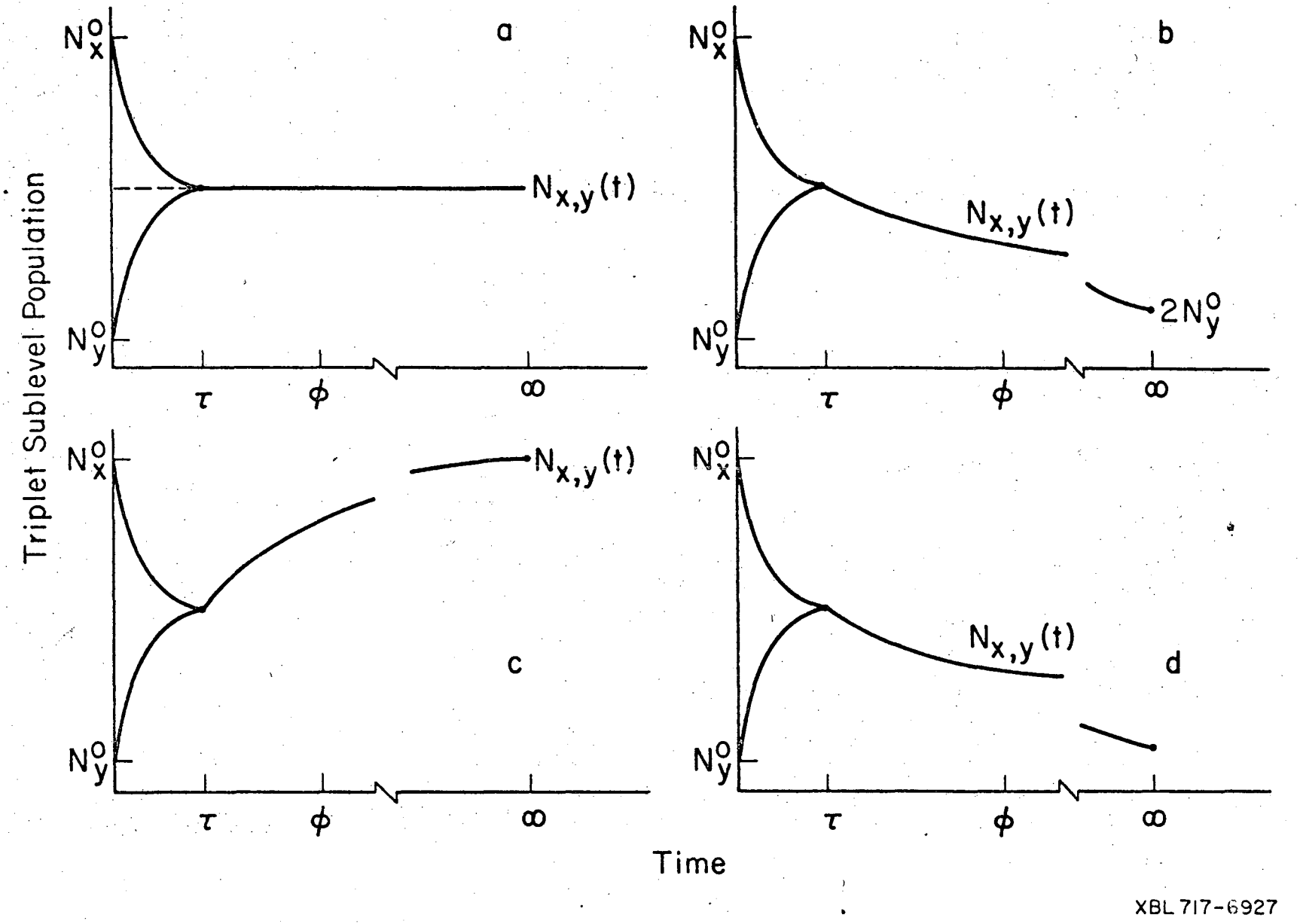

XBL 717-6927

Fig. 5

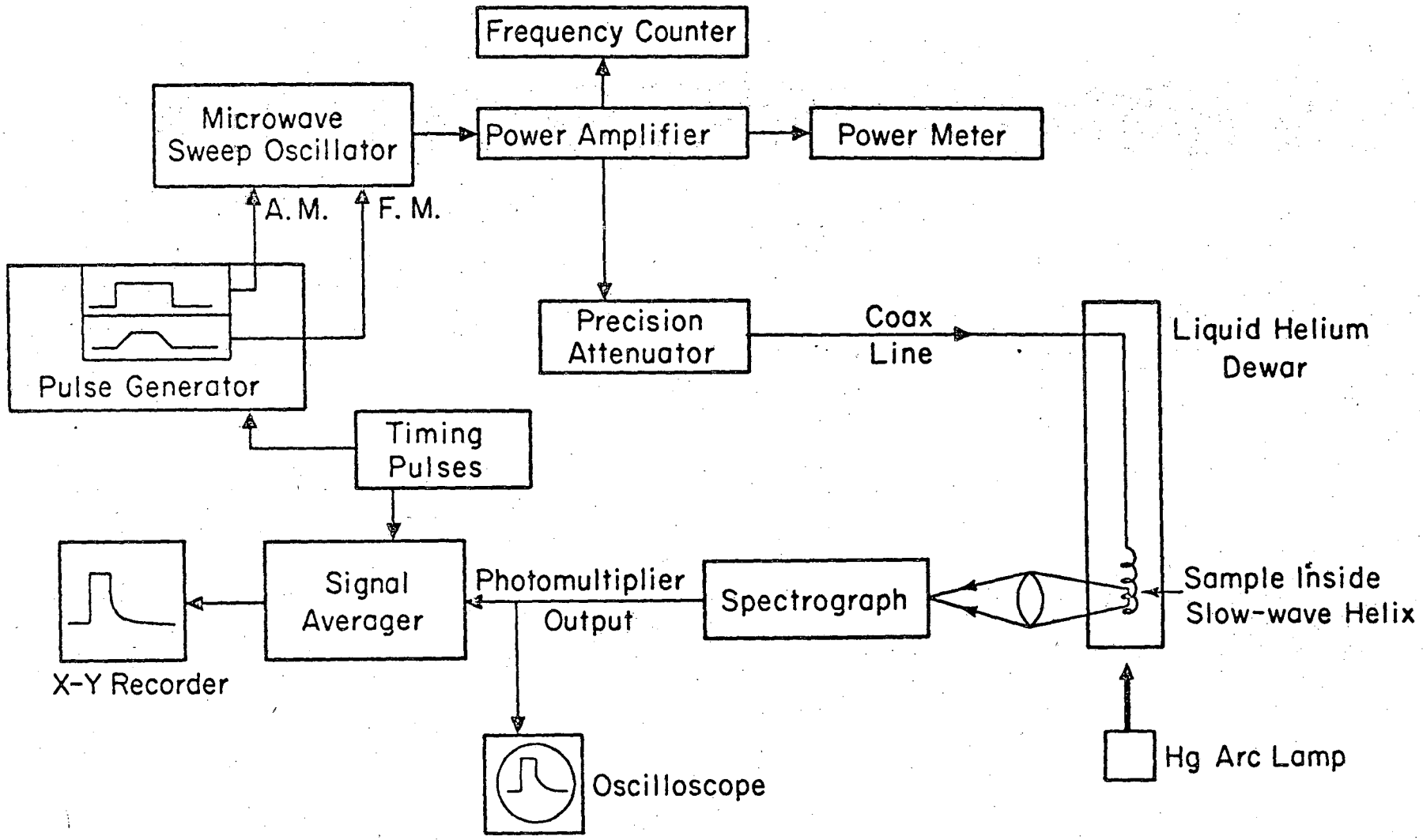

INSTRUMENTAL ARRANGEMENT

XBL 716-6898

Fig. 6

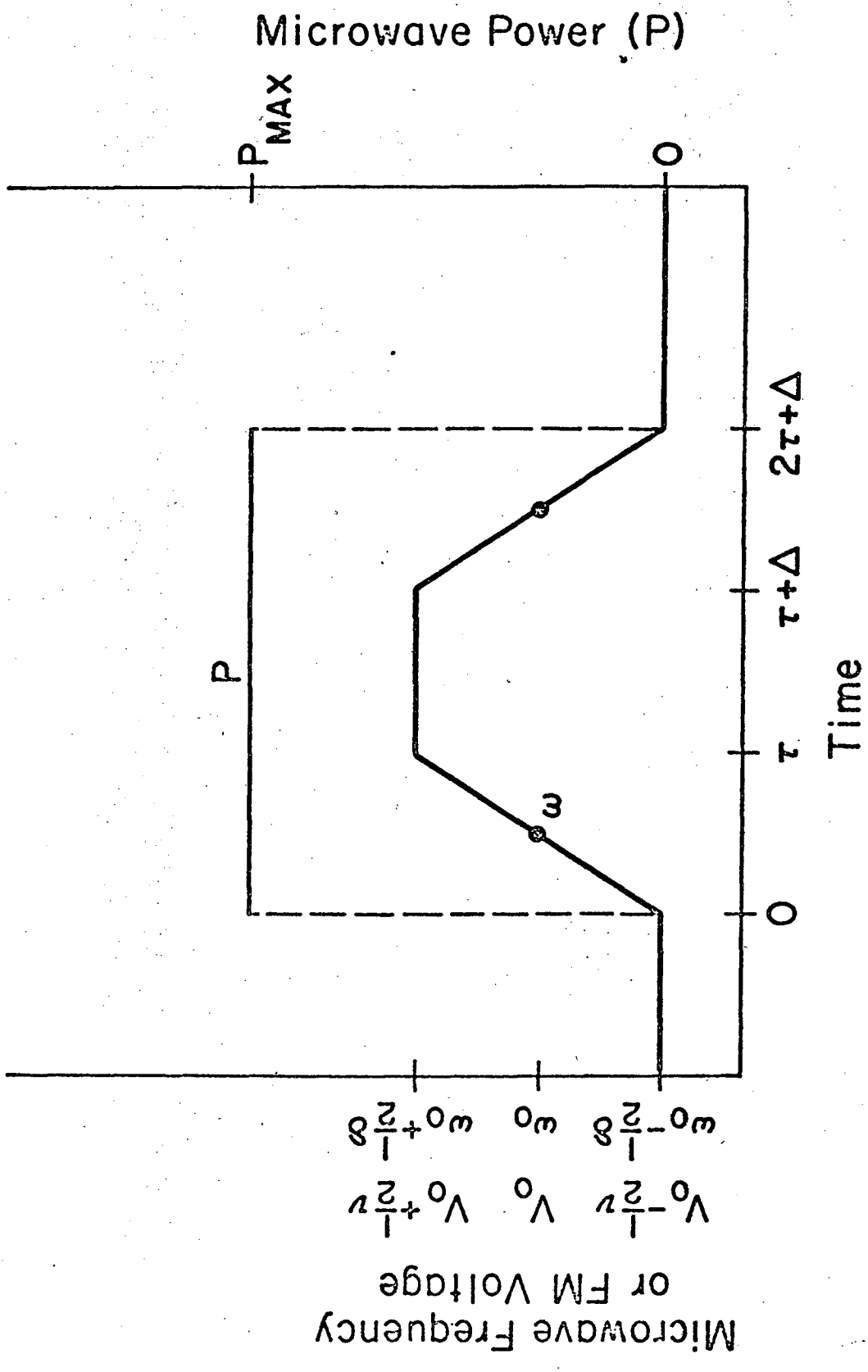

XBL 716-6895

Fig. 7

TECHNICAL INFORMATION DIVISION
LAWRENCE BERKELEY LABORATORY
UNIVERSITY OF CALIFORNIA
BERKELEY, CALIFORNIA 94720